Tracing complex equilibrium paths of elastic structures by an improved 'Admissible Directions Cone' method

Paolo S. Valvo* and Salvatore S. Ligarò

Department of Structural Engineering
University of Pisa, Via Diotisalvi 2, I-56126 Pisa, Italy
e-mail: p.valvo@ing.unipi.it, s.ligaro@ing.unipi.it

Key words: equilibrium stability, path-tracing strategy, bifurcation, snap-through

Abstract
The post-critical behaviour of a slender elastic structure under an assigned system of proportional loads is wholly disclosed by means of its equilibrium path. To achieve a uniformly accurate tracing of the path, incremental-iterative strategies use a variable step-length to adapt the sampling of points to the complexity of the curve. This paper illustrates a revised formulation of the 'Admissible Directions Cone' method, a particular arc-length procedure, in which an inequality constraint is added to the standard set of governing equations to limit the change in angle experienced by the tangent to the path in a step. The effectiveness of the method is demonstrated in severe circumstances, such as the examples presented here, concerning simple kinematically indeterminate truss structures, whose equilibrium paths are nevertheless characterised by *bifurcation points at the origin* and *zero-load secondary branches*.

1 Introduction

Loss of equilibrium stability is no doubt the typical failure mode for a number of prevailingly compressed structural typologies, such as slender metal arches, continuum or reticulated shells, thin vaults and domes. This insidious sort of failure is destined to become more and more frequent as the use of new high-performance materials spreads. In these cases, the assessment of the ultimate bearing capacity of a structure cannot be limited to the mere determination of a buckling or snapping load. Instead, a complete non-linear analysis is needed, since even apparently simple structural systems often hide a surprisingly complex post-critical behaviour.

The mechanical response of an elastic structure under proportional loading can be concisely represented by its *equilibrium path*, namely, the set of curves in the $n+1$-dimensional space spanned by the *load multiplier*, λ, and the *generalised displacements*, q_1, q_2, …, q_n, of the discrete model. Each point of the path represents an equilibrium configuration assumed by the structure [1, 2].

Arc-length methods assume the *curvilinear abscissa*, s, as the representation parameter and perform a sampling of points at increasing values of it [3, 4, 5]. The early formulations used a constant parameter increment, or *step-length*, but this turns out to be inadequate when long and winding paths have to be traced accurately [6, 7, 8]. In these cases, according to the degree of imperfection of the structural system, the paths exhibit a wide gamut of post-critical behaviour, including simple and multiple bifurcation, snapping, sharp turning points, loops and so on. So, small step-lengths lead to inefficient and demanding computation, while large values may cause the algorithm to fail along arcs of greater curvature or in the neighbourhood of a bifurcation, due to undesired jumps onto the bifurcated branch.

In [9], a method was presented where the step-length is suitably reduced whenever the changes in direction experienced by the unit tangent vector are greater than a given value. To this aim, an inequality constraint was added to the standard set of governing equation, in order to force the secant vector at each incremental step to lie inside a *cone of admissible directions*.

The paper presents a revised formulation of the above method, where the step-length is either reduced or increased according to the complexity of the curve. The versatility of the method in tracing correctly the path in presence of sharp turning points or unexpected bifurcation points, permits the analyst to focus his attention to the mechanical aspects of the problem. The effectiveness of the method is demonstrated in severe circumstances, such as the examples presented here, concerning simple kinematically indeterminate truss structures, whose equilibrium paths are nevertheless characterised by *bifurcation points at the origin* and *zero-load secondary branches* [10].

2 Path-tracing strategy

Within an FEM framework, the configurations assumed by an elastic structure under a set of *nodal loads* $\lambda\mathbf{p} = \lambda\,[\,p_1, p_2, \ldots, p_n\,] \in \mathbb{R}^n$, where λ is the *load multiplier*, are described by a vector of *nodal displacements* $\mathbf{q} = [\,q_1, q_2, \ldots, q_n\,] \in \mathbb{R}^n$, which are solutions of the non-linear equilibrium equation set

$$\mathbf{f}\,(\lambda;\,\mathbf{q}) = \mathbf{K}(\mathbf{q})\,\mathbf{q} - \lambda\mathbf{p} = \mathbf{0}, \tag{1}$$

where $\mathbf{K}(\mathbf{q}) \in \mathbb{R}^{n \times n}$ is the *secant stiffness matrix* of the structure.

The solutions of equations (1) can be plotted as the points of the *equilibrium path* of the structure in the $n+1$-dimensional space with co-ordinates $t_0 = \lambda$, $t_1 = q_1$, $t_2 = q_2$, …, $t_n = q_n$.

The *origin* $\mathbf{t}_{(0)} = [\,\lambda_{(0)};\,\mathbf{q}_{(0)}\,] = [\,0;\,\mathbf{0}\,]$ always belongs to the path. By convention, the curve passing through it is called the *primary branch*; other curves, if any, are said to be *secondary branches*. Starting from $\mathbf{t}_{(0)}$, arc-length methods represent the path as a broken line of chords whose endpoints, $\mathbf{t}_{(1)}$, $\mathbf{t}_{(2)}$, …, $\mathbf{t}_{(K)}$, …, correspond to increasing values of the curvilinear abscissa, $s_{(1)}$, $s_{(2)}$, …, $s_{(K)}$, …

2.1 The incremental-iterative procedure

Each incremental step starts from a known point location $\mathbf{t}_{(K)} = [\ \lambda_{(K)};\ \mathbf{q}_{(K)}\ ]$, corresponding to the abscissa $s_{(K)}$. The *unit tangent vector* to the path at the same point, $\dot{\mathbf{t}}_{(K)} = [\ \dot{\lambda}_{(K)};\ \dot{\mathbf{q}}_{(K)}\ ]$, can be determined by solving the so-called first order static perturbation problem [1, 2] (here and in the following, an upper dot denotes differentiation with respect to the curvilinear abscissa *s*)

$$
\left[
\begin{array}{c|c}
\dot{\lambda}_{(K)} & (\dot{\mathbf{q}}_{(K)})^T \\
\hline
-\mathbf{p} & \mathbf{K_T}(\mathbf{q}_{(K)})
\end{array}
\right]
\dot{\mathbf{t}}_{(K)} =
\begin{bmatrix} 1 \\ \hline \mathbf{0} \end{bmatrix},
\tag{2}
$$

where $\mathbf{K_T}(\mathbf{q}) = \partial[\ \mathbf{K}(\mathbf{q})\mathbf{q}\ ]/\partial\mathbf{q} \in \mathbb{R}^{n \times n}$ is the *tangent stiffness matrix* of the structure.

At each step, the problem consists of finding the point $\mathbf{t} = [\ \lambda;\ \mathbf{q}\ ] = \mathbf{t}_{(K+1)}$ or, alternatively, the *secant vector*, $\Delta\mathbf{t}_{(K)} = [\ \Delta\lambda_{(K)};\ \Delta\mathbf{q}_{(K)}\ ] = \mathbf{t} - \mathbf{t}_{(K)}$, relative to the subsequent value of the parameter $s = s_{(K)} + \Delta s_{(K)} = s_{(K+1)}$, where $\Delta s_{(K)}$ is the assigned step-length. In the present formulation, the abscissa increment is approximated by the length of the secant vector, so the following *auxiliary equation*,

$$
f_0(\mathbf{t};s) = (\mathbf{t} - \mathbf{t}_{(K)})^2 - (s - s_{(K)})^2 = \Delta\mathbf{t}_{(K)}{}^2 - \Delta s_{(K)}{}^2 = 0,
\tag{3}
$$

which requires the sought point $\mathbf{t}$ to belong to the sphere of radius $\Delta s_{(K)}$ and centre at $\mathbf{t}_{(K)}$, is added to the equilibrium equations (1), yielding the *augmented system* [3, 4, 5]

$$
\begin{cases}
f_0(\lambda;\mathbf{q};s) = (\lambda - \lambda_{(K)})^2 + (\mathbf{q} - \mathbf{q}_{(K)})^2 - \Delta s_{(K)}{}^2 = 0, \\
\mathbf{f}(\lambda;\mathbf{q}) = \mathbf{K}(\mathbf{q})\mathbf{q} - \lambda\mathbf{p} = \mathbf{0}.
\end{cases}
\tag{4}
$$

A predictor-corrector scheme, based on the Newton-Raphson method, is applied to obtain $\Delta\mathbf{t}_{(K)}$ from system (4). The first estimate is given by the linear *predictor*

$$
\Delta\mathbf{t}_{(K,0)} = \Delta s_{(K)}\dot{\mathbf{t}}_{(K)},
\tag{5}
$$

while improved estimates, $\Delta\mathbf{t}_{(K,1)}$, $\Delta\mathbf{t}_{(K,2)}$, …, $\Delta\mathbf{t}_{(K,H)}$, …, are obtained by repeated iterations. At each iteration, the *corrector* $\delta\,\mathbf{t}_{(K,H)}$ is determined by solving the following equation set

$$
\left[
\begin{array}{c|c}
2\Delta\lambda_{(K,H)} & 2(\Delta\mathbf{q}_{(K,H)})^T \\
\hline
-\mathbf{p} & \mathbf{K_T}(\mathbf{q}_{(K+1,H)})
\end{array}
\right]
\delta\,\mathbf{t}_{(K,H)} = -
\left[
\begin{array}{c}
f_0(\lambda_{(K+1,H)};\mathbf{q}_{(K+1,H)};s) \\
\hline
\mathbf{f}(\lambda_{(K+1,H)};\mathbf{q}_{(K+1,H)})
\end{array}
\right],
\tag{6}
$$

so the updated secant vector becomes $\Delta\mathbf{t}_{(K,H+1)} = \Delta\mathbf{t}_{(K,H)} + \delta\,\mathbf{t}_{(K,H)}$, while the updated point location is determined after the secant vector has been further scaled to fit the spherical constraint (3)

$$
\mathbf{t}_{(K+1,H+1)} = \mathbf{t}_{(K)} + \Delta s_{(K)}\,\Delta\mathbf{t}_{(K,H+1)}\big/\big\|\Delta\mathbf{t}_{(K,H+1)}\big\|.
\tag{7}
$$

Iterations are continued until $\big\|\delta\,\mathbf{t}_{(K,H)}\big\|$ is smaller than a given tolerance, *TOL*.

2.2 Solution strategy at regular points

Systems (2) and (6) are both solved through the diagonalisation of the tangent stiffness matrix, carried out by means of the classic Jacobi algorithm. In fact, since $\mathbf{K_T}$ is a symmetric and real-valued matrix, then *n* mutually orthogonal *eigenvectors* exist, $\mathbf{a}_1$, $\mathbf{a}_2$, …, $\mathbf{a}_n$, such that

$$
\mathbf{K_T}\mathbf{a}_i = \omega_i\mathbf{a}_i, \quad i = 1,2,...,n,
\tag{8}
$$

relative to *n* real *eigenvalues*, $\omega_1 \leq \omega_2 \leq \ldots \leq \omega_n$.

By virtue of equations (8), and expressing $\dot{\mathbf{q}}$ and $\delta\,\mathbf{q}$ with respect to the eigenvector basis,

$$\dot{\mathbf{q}} = \sum_{i=1}^{n} \dot{u}_i \mathbf{a}_i\,, \qquad\qquad \delta\,\mathbf{q} = \sum_{i=1}^{n} \delta\,u_i \mathbf{a}_i\,, \qquad\qquad \text{(9a,b)}$$

system (2) can be put in the form (subscripts K and H are here omitted for simplicity)

$$\begin{cases} \dot{\lambda}^2 + \sum_{i=1}^{n} \dot{u}_i^{\;2} = 1, \\ -\dot{\lambda}\,\mathbf{p}^T \mathbf{a}_i + \omega_i \dot{u}_i = 0, \quad i = 1,2,\ldots,n, \end{cases} \qquad (10)$$

while system (6) becomes

$$\begin{cases} 2\Delta\lambda\,\delta\,\lambda + 2\Delta\mathbf{q}^T \sum_{i=1}^{n} \delta\,u_i \mathbf{a}_i = 1, \\ -\lambda\,\mathbf{p}^T \mathbf{a}_i + \omega_i \delta\,u_i = -\mathbf{f}^T \mathbf{a}_i, \quad i = 1,2,\ldots,n. \end{cases} \qquad (11)$$

At *regular points* of the path, all eigenvalues are non-zero. Thus, the unit tangent vector can be determined by solving first system (10) as follows

$$\begin{cases} \dot{\lambda} = \pm\left[1 + \sum_{i=1}^{n} (\mathbf{p}^T \mathbf{a}_i / \omega_i)^2\right]^{-1/2}, \\ \dot{u}_i = \dot{\lambda}\,\mathbf{p}^T \mathbf{a}_i / \omega_i\,, \quad i = 1,2,\ldots,n, \end{cases} \qquad (12)$$

and then making use of equations (9a) to deduce $\dot{\mathbf{q}}$ (the choice of the sign will be discussed later). Likewise, the corrector can be obtained by solving first system (11) to yield

$$\begin{cases} \delta\,\lambda = \left[1/2\,(\Delta s^2 - \Delta\lambda^2 - \Delta\mathbf{q}^2) + \mathbf{f}^T\left(\sum_{i=1}^{n} \mathbf{a}_i \mathbf{a}_i^{\;T} / \omega_i\right)\!\Delta\mathbf{q}\right]\!\Big/\!\left[\Delta\lambda + \mathbf{f}^T\left(\sum_{i=1}^{n} \mathbf{a}_i \mathbf{a}_i^{\;T} / \omega_i\right)\!\Delta\mathbf{q}\right], \\ \delta\,u_i = (\delta\,\lambda\,\mathbf{p} - \mathbf{f})^T \mathbf{a}_i / \omega_i\,, \quad i = 1,2,\ldots,n, \end{cases} \qquad (13)$$

and then making use of equations (9b) to deduce $\delta\,\mathbf{q}$.

2.3 Critical points

At simple *critical points*, one eigenvalue is null, say $\omega_j = 0$, while $\omega_i \neq 0$ for $i \neq j$. Solution of system (10) requires two cases to be considered [6, 7, 8]:
a) if $\mathbf{p}^T \mathbf{a}_j \neq 0$ then the point is a *limit point*: a unique tangent to the path exist and is furnished by

$$\begin{cases} \dot{\lambda} = 0, \\ \dot{u}_i = 0, \quad i = 1,2,\ldots,n, \quad i \neq j, \\ \dot{u}_j = \pm 1; \end{cases} \qquad (14)$$

while the Newton-Raphson corrector results from

$$\begin{cases} \delta\,\lambda = \mathbf{f}^T \mathbf{a}_j / \mathbf{p}^T \mathbf{a}_j \\ \delta\,u_i = (\delta\,\lambda\,\mathbf{p} - \mathbf{f})^T \mathbf{a}_i / \omega_i\,, \quad i = 1,2,\ldots,n, \quad i \neq j, \\ \delta\,u_j = \left[1/2\,(\Delta s^2 - \Delta\lambda^2 - \Delta\mathbf{q}^2) - \Delta\lambda\,\delta\,\lambda - \Delta\mathbf{q}^T \sum_{i=1\,(i\neq j)}^{n} \delta\,u_i \mathbf{a}_i\right]\!\Big/\Delta\mathbf{q}^T \mathbf{a}_j\,; \end{cases} \qquad (15)$$

and then making use of equations (9b) to deduce $\delta\,\mathbf{q}$.

b) if $\mathbf{p}^T\mathbf{a}_j = 0$ then the point is a *bifurcation point*: for a symmetric bifurcation, two distinct tangents to the path are present

$$
\begin{cases}
\dot{\lambda} = \pm\left[1 + \sum_{i=1\,(i\neq j)}^{n}\left(\mathbf{p}^T\mathbf{a}_i/\omega_i\right)^2\right]^{-1/2}, \\
\dot{u}_i = \dot{\lambda}\ \mathbf{p}^T\mathbf{a}_i/\omega_i, \quad i = 1,2,...,n, \quad i \neq j, \\
\dot{u}_j = 0;
\end{cases}
\quad \text{and} \quad
\begin{cases}
\dot{\lambda} = 0, \\
\dot{u}_i = 0, \quad i = 1,2,...,n, \quad i \neq j, \quad \text{(16a,b)}\\
\dot{u}_j = \pm 1;
\end{cases}
$$

In this case, system (11) has no solutions at all, so that standard arc-length methods fail. However, although this event may appear rather exceptional, as it requires the current iterate to fall exactly on a bifurcation point, in practice it is sufficient that iterations are carried out *in the neighbourhood* of a bifurcation point for numerical difficulties to arise. In fact, when the minimum eigenvalue approaches zero, the correctors given by (13) become very large in norm. As a consequence, the secant vector undergoes sudden changes in both norm and direction, with the risk of erroneous jumps of the algorithm onto a bifurcated branch. This possibility can be prevented as explained in the following.

3 The cone of admissible directions

3.1 Basic idea and definition

The basic idea consists of setting an upper limit to the change in angle experienced by the unit tangent vector within each incremental step. To this aim, the concept of the osculating circle is suitably exploited, in order to fit the proposed strategy within the context of standard arc-length methods. In what follows, a brief outline of the algorithm is given. Details can be found in the original paper [9].
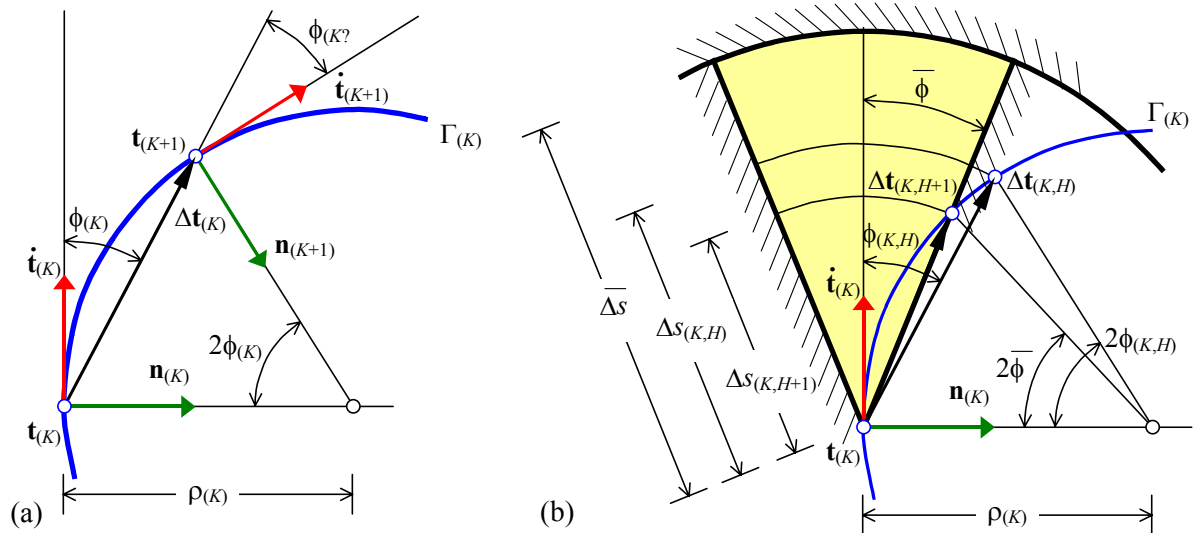

Figure 1: The cone of admissible directions

Figure 1a shows two consecutive points on the path, $\mathbf{t}_{(K)}$ and $\mathbf{t}_{(K+1)}$, their respective unit tangent vectors, $\dot{\mathbf{t}}_{(K)}$ and $\dot{\mathbf{t}}_{(K+1)}$, and unit principal normal vectors, $\mathbf{n}_{(K)}$ and $\mathbf{n}_{(K+1)}$. The above two points are supposed to be close enough each other, so that the path segment connecting them can be approximated by a small arc of the osculating circle, $\Gamma_{(K)}$, whose radius is $\rho_{(K)}$. The angle formed by $\dot{\mathbf{t}}_{(K)}$ and $\dot{\mathbf{t}}_{(K+1)}$ is twice the

angle, $\phi_{(K)}$, between $\dot{\mathbf{t}}_{(K)}$ and $\Delta\mathbf{t}_{(K)}$. Hence, limiting the angle change experienced by $\dot{\mathbf{t}}$ during the incremental step K is equivalent to imposing the following inequality constraint

$$\phi_{(K)} \leq \overline{\phi} \tag{17}$$

which defines the *cone of admissible directions*, within which the secant vector, $\Delta\mathbf{t}_{(K)}$, must fall. This cone has vertex at $\mathbf{t}_{(K)}$, axis $\dot{\mathbf{t}}_{(K)}$ and half-cone angle $\overline{\phi}$ (Figure 1b).

3.2 Step reduction

At the end of iterative cycle H, the angle between $\Delta\mathbf{t}_{(K,H)}$ and $\dot{\mathbf{t}}_{(K)}$ is computed from

$$\cos\phi_{(K,H)} = \left(\Delta\mathbf{t}_{(K,H)} \cdot \dot{\mathbf{t}}_{(K)}\right) \big/ \left\|\Delta\mathbf{t}_{(K,H)}\right\| \tag{18}$$

When $\phi_{(K,H)} > \overline{\phi}$, the current step-length $\Delta s_{(K,H)}$ needs to be reduced to

$$\Delta s_{(K,H+1)} = \sin\overline{\phi} \big/ \sin\phi_{(K,H)} \, \Delta s_{(K,H)}, \tag{19}$$

in order to satisfy the constraint (17); moreover, an updated secant vector is determined as the one joining point $\mathbf{t}_{(K)}$ to the point where the cone of admissible directions intersects the osculating circle,

$$\Delta\mathbf{t}_{(K,H+1)} = (\sin\overline{\phi} \big/ \sin\phi_{(K,H)})^2 \, \Delta\mathbf{t}_{(K,H)} + \Delta s_{(K,H+1)} \sin(\phi_{(K,H)} - \overline{\phi}) \big/ \sin\phi_{(K,H)} \, \dot{\mathbf{t}}_{(K)}. \tag{20}$$

3.3 Step increase

After convergence has been achieved, the half-cone angle $\phi_{(K)}$ is *a posteriori* calculated from

$$\cos\phi_{(K)} = \dot{\mathbf{t}}_{(K)} \cdot \dot{\mathbf{t}}_{(K+1)} \tag{21}$$

Then, provided that $\phi_{(K)} < \overline{\phi}$, the step-length for the subsequent incremental step, $\Delta s_{(K+1)}$, is increased to the maximum value which does not violate the imposed constraint,

$$\Delta s_{(K+1)} = \min\left\{\sin\overline{\phi} \big/ \sin\phi_{(K)} \, \Delta s_{(K)}, \quad \overline{\Delta s}\right\}, \tag{22}$$

where $\overline{\Delta s}$ is the initial step-length, assigned at the beginning of the incremental-iterative procedure.

4 Applications

4.1 A crank gear model

In order to illustrate the versatility of the method, a crank gear model was analysed (Figure 2). Although seemingly simple, this example represents a severe test for most path-tracing algorithms: in fact, due to the possibility of a finite mechanism, the equilibrium path features a whole branch characterised by $\lambda = 0$ and $\dot{\lambda} = 0$ starting from the origin.

Figures 3a and 3b show the equilibrium path in the u_1-λ plane and u_2-v_2 plane, respectively, obtained with the following numerical values: $\overline{\Delta s} = 50$ cm, $\overline{\phi} = 0.10$ rad, $TOL = 10^{-6}$.
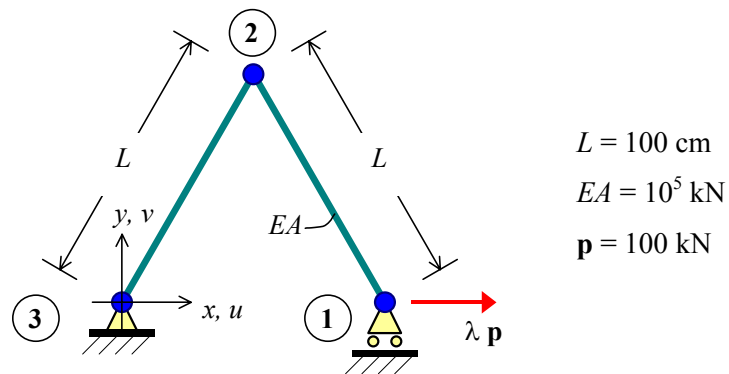
Figure 2: Crank gear: the model

$L = 100$ cm
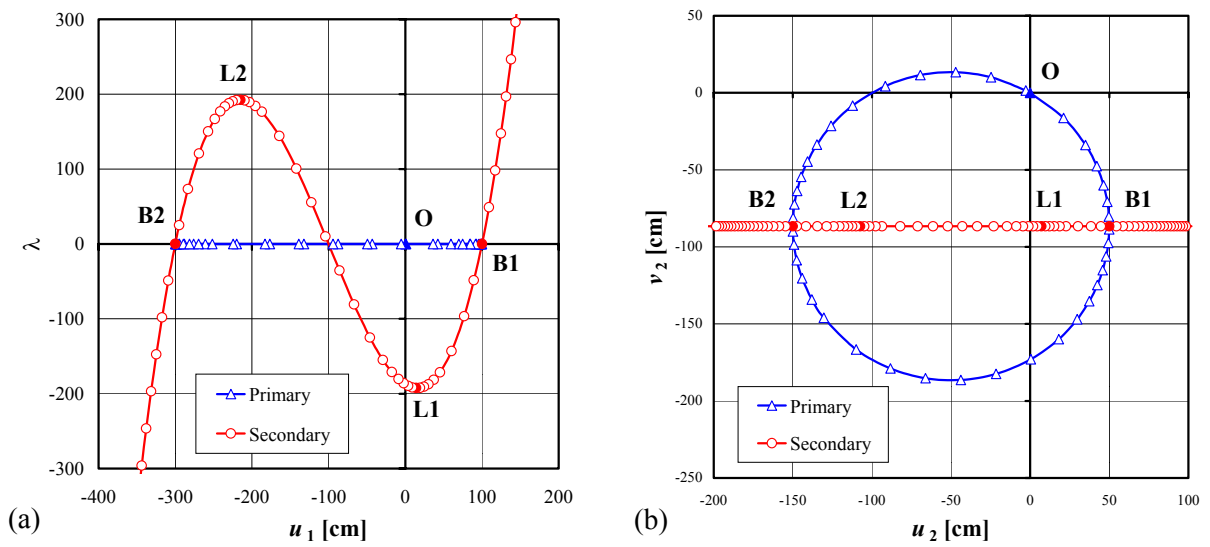$EA = 10^5$ kN
$\mathbf{p} = 100$ kN

(a)

(b)

Figure 3: Crank gear: the equilibrium path

4.2 Two reticulated towers

Next, the two reticulated towers shown in Figure 4 were analysed. In both cases, the joints of the lower hexagon were fixed, while the upper ones were subjected to vertical loads with $\mathbf{p} = 200$ kN.
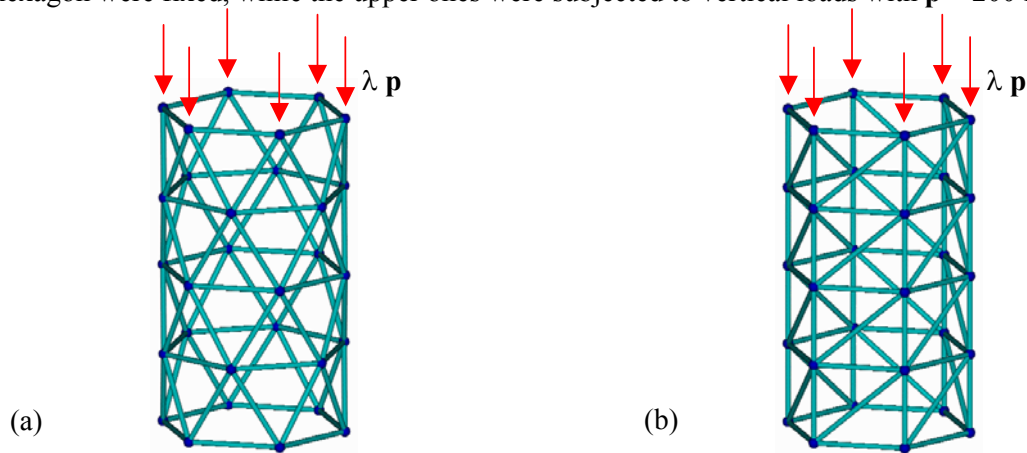

(a)

(b)

Figure 4: Two reticulated towers

The symmetrically-braced reticulated tower (Figure 4a) is kinematically indeterminate [10]. Therefore, the origin of the λ-**q** space turns out to be a bifurcation point and the corresponding secondary branch is characterised by $\lambda = 0$ and $\dot{\lambda} = 0$. This is shown in Figures 5a and 5b, where the equilibrium path in the λ-w_{28} plane and u_{28}-w_{28} plane, respectively, is represented (Joint 28 belongs to the upper hexagon). The numerical values $\overline{\Delta s} = 50$ cm, $\overline{\dot{\phi}} = 0.10$ rad, $TOL = 10^{-6}$ were again used.
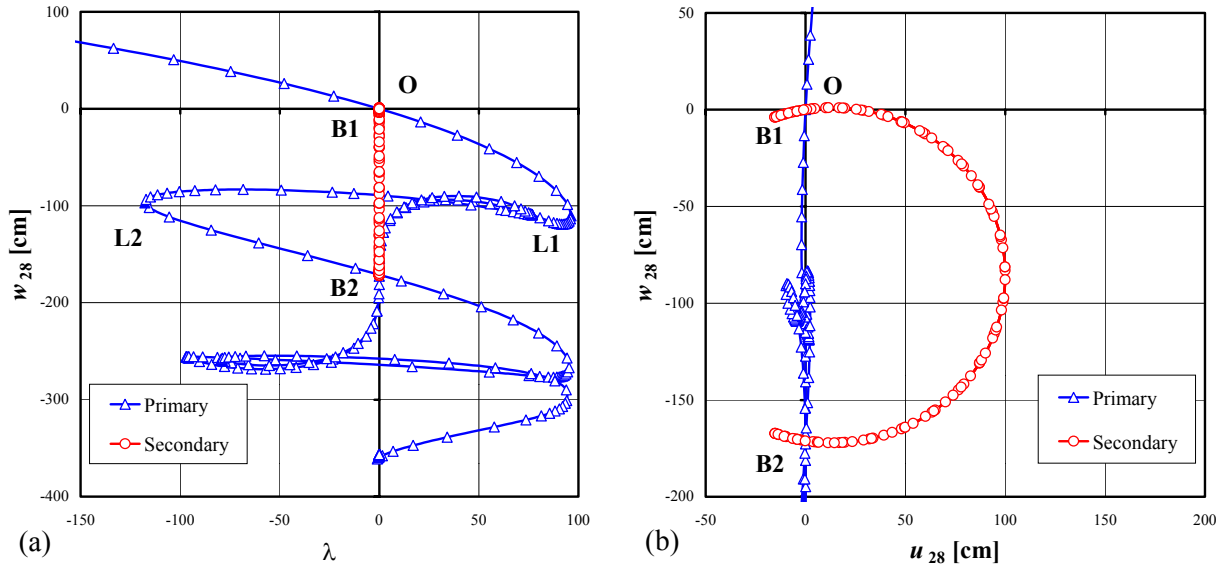
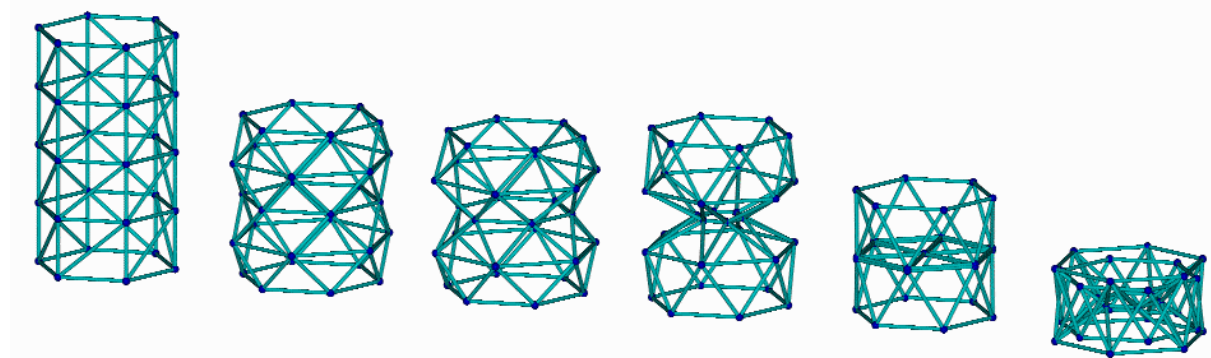Figure 5: Symmetrically-braced reticulated tower: equilibrium path

Figure 6: Symmetrically-braced tower: equilibrium configurations along the primary path
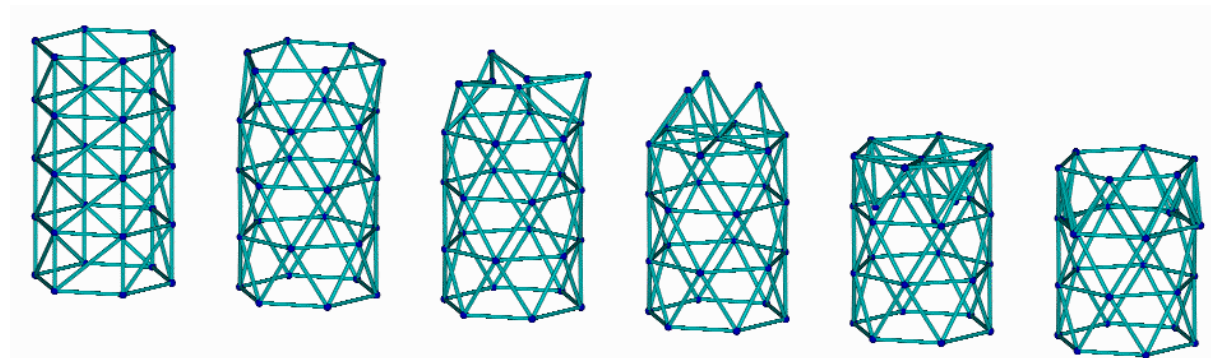

Figure 7: Symmetrically-braced tower: equilibrium configurations along the secondary path

Figures 8a and 8b represent the equilibrium path in the λ-w_{28} plane and u_{28}-w_{28} plane, respectively, for the spirally-braced reticulated tower. In this case, a bifurcation point was detected very close to the origin. The corresponding secondary branch is depicted in the figures below.
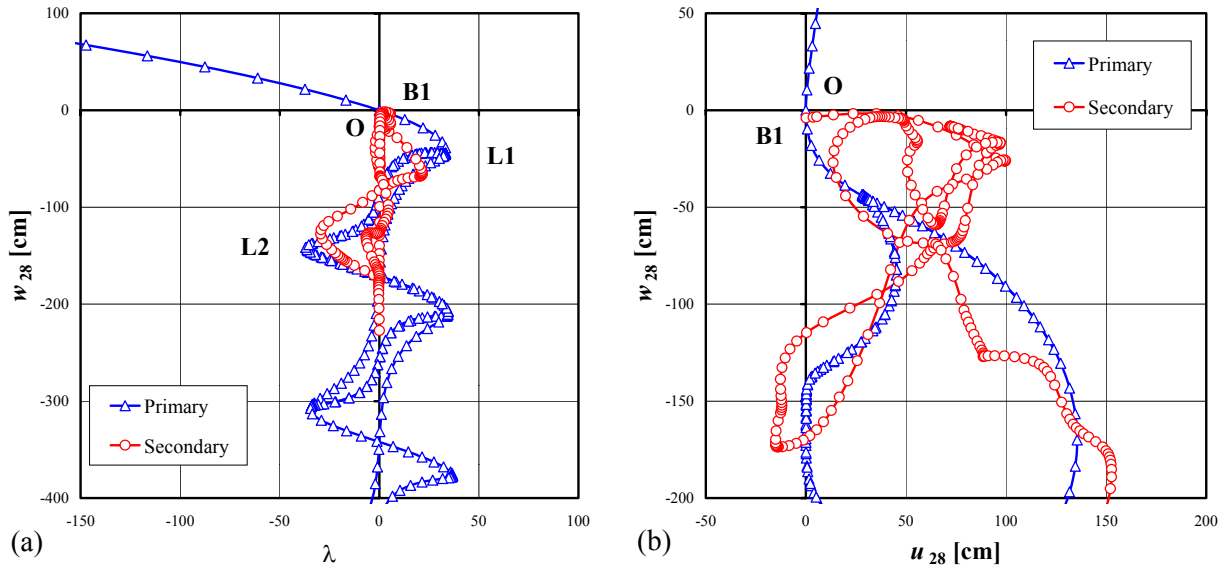

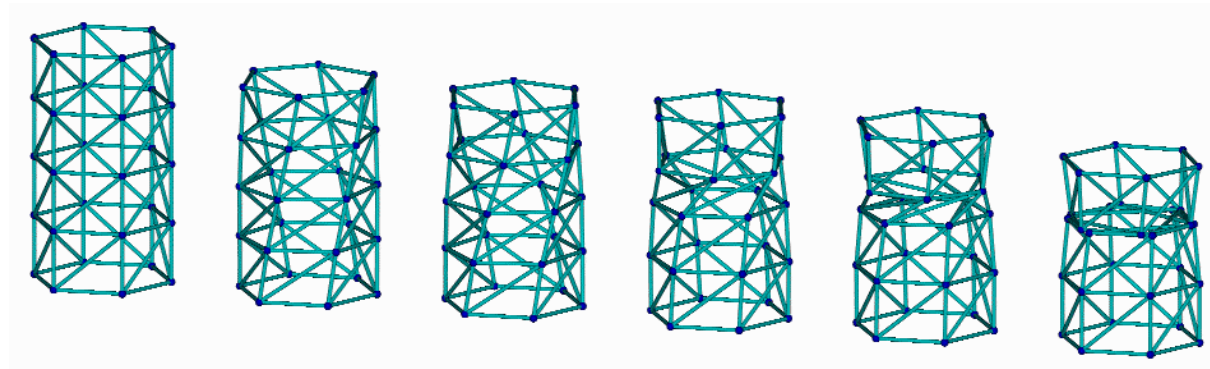Figure 8: Spirally-braced reticulated tower: equilibrium path

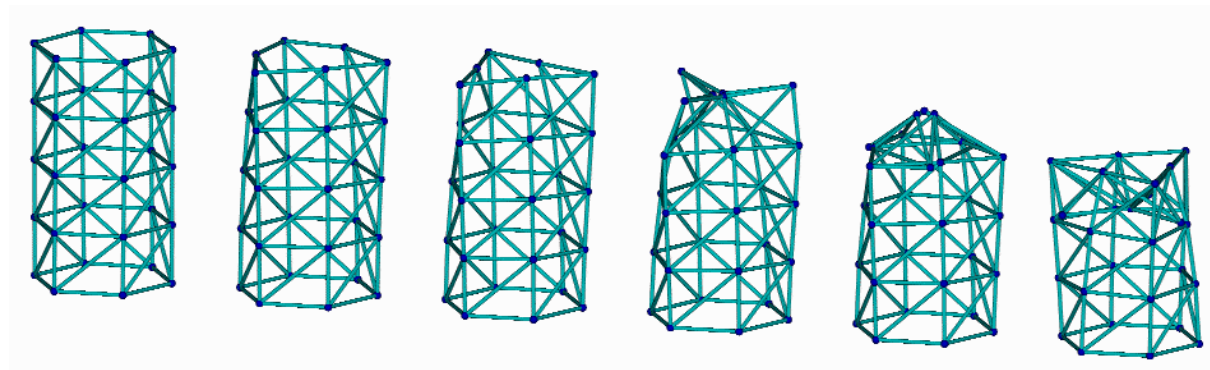Figure 9: Spirally-braced tower: equilibrium configurations along the primary path

Figure 10: Spirally-braced tower: equilibrium configurations along the secondary path

5 Conclusion

The paper illustrated a revised version of the 'Admissible Directions Cone' method, a path-tracing strategy, in which the parameter increment is step-wise adapted to the complexity of the curve. The inclusion of a new criterion for either reducing or increasing the step-length has improved significantly the computational efficiency and effectiveness of the algorithm with respect to previous formulations. The method proved its potential in tracing complex equilibrium paths endowed with sharp turning points or unexpected bifurcation points.

As a first test, the non-linear behaviour of a simple crank gear model was analysed. Its primary and secondary branches were traced completely. Due to the kinematical indeterminacy of this structural system, the primary branch develops entirely under zero applied load.

Furthermore, two reticulated towers with different bracing schemes were considered. In the case of a symmetric bracing, the equilibrium path featured a bifurcation point at the origin and a zero-load secondary branch (finite mechanism). *Vice versa*, in the case of a spiral bracing, a bifurcation point was detected very close to the origin. Although the difference in the bracing schemes might appear very slight according to linear theory, nevertheless their non-linear post-critical behaviour turned out to be totally different.

References

[1] M. J. Sewell, *A general theory of equilibrium paths through critical points*, Proc. Roy. Soc., A. 306 (1968), 201-238.

[2] J. M. T. Thompson, G. W. Hunt, *Elastic instability phenomena*, John Wiley & Sons Ltd., Chichester, England (1984).

[3] E. Riks, *An incremental approach to the solution of snapping and buckling problems*, Int. J. Sol. Struct., 15, (1979), 529-551.

[4] M. A. Crisfield, *A fast incremental/iterative solution procedure that handles "snap-through"*, Comput. Struct., 13, (1981), 55-62.

[5] R. Kouhia, M. Mikkola, *Tracing the equilibrium path beyond simple critical points*, Int. J. Num. Meth. Eng., 28, (1989), 2933-2941.

[6] P. Wriggers, W. Wagner, C. Miehe, *A quadratically convergent procedure for the calculation of stability points in finite elements analysis*, Comp. Meths. Appl. Mech. Eng., 70, (1988), 329-347.

[7] P. Wriggers, J. C. Simo, *A general procedure for the direct computation of turning and bifurcation points*, Int. J. Num. Meth. Eng., 30, (1990), 155-176.

[8] A. Erikson, R. Kouhia, *On step size adjustments in structural continuation problems*, Comput. Struct., 55, (1995), 495-505.

[9] S. Ligarò, P. Valvo, *A self-adaptive strategy for uniformly accurate tracing of the equilibrium paths of elastic reticulated structures*, Int. J. Num. Meth. Eng., 46, (1999), 783-804.

[10] T. Tarnai, *Simultaneous static and kinematic indeterminacy of space trusses with cyclic symmetry*, Int. J. Sol. Struct., 16, (1980), 347-359.